



ISSN: 0067-2904

## Bio Synthesis, Characterization, and Evaluation of the Anticancer Activity of Gold and Silver Nanoparticles and Their Polyacetal Nanocomposite

Dalia J. Hadi, Maha A. Younus\*

Department of Chemistry, College of Education for Pure Science (Ibn Al-Haitham), University of Baghdad, Baghdad, Iraq

Received: 21/6/2023

Accepted: 13/11/2023

Published: 30/12/2024

### Abstract

This study synthesized polyacetal from the reaction of polyvinyl alcohol with para-nitrobenzaldehyde. Polyacetal/polyvinylpyrrolidone polymer blends were prepared using solution casting. Gold nanoparticles (AuNPs) and silver nanoparticles (AgNPs) were biosynthesized using onion peel extract as the reducing agent. Nanocomposites were fabricated by blending polyacetal/PVP with AuNPs and AgNPs at different ratios. XRD and FESEM characterized the AuNPs and AgNPs. FTIR, FESEM, TGA, and DSC characterized the polyacetal, polymer blends, and nanocomposites. DSC and TGA confirmed the improved thermal stability of the polymer blends and nanocomposites. Nanocomposites demonstrated higher efficacy in inhibiting lung cancer cell lines compared to the blends alone.

**Keywords:** Anti-cancer cell line, PVA, PVP, Polyacetal, Nanocomposite.

## التحضير الحيوي، التشخيص والفعالية المضادة للسرطان لدقائق الذهب والفضة النانوية والمترابكات النانوية للبولي اسيتال

داليا هادي , مها يونس\*

قسم الكيمياء، كلية التربية للعلوم الصرفة (ابن الهيثم)، جامعة بغداد، بغداد، العراق

### الخلاصة

في هذه الدراسة ، تم تحضير بولي أسيتال من تفاعل بولي فاينيل الكحول مع بارا نايترز بنزالديهايد. تم تحضير مزيج البوليمر من بولي اسيتال / بولي فاينيل بريليدون بطريقه خلط المحاليل. تم التحضير الحيوي لدقائق النانوية للذهب والدقائق النانوية للفضة بواسطة مستخلصات قشور البصل كعامل مختزل. المترابكات النانوية حضرت من خلط بولي اسيتال / بولي فاينيل بريليدون مع دقائق الذهب والفضة النانوية وبنسب مختلفة. طيف حيود الاشعة السينية والمجهر الالكتروني الماسح شخص دقائق الذهب والفضة النانوية المحضرة. مطيافية الاشعة تحت الحمراء والمجهر الالكتروني الماسح والتحليل الحراري شخصت البولي اسيتال وخلائط البوليمر والمترابكات النانوية المحضرة. التحليل المسح الحراري التفاضلي والتحليل الحراري الوزني اثبتت الاستقرار الحراري للخلائط والمترابكات المحضرة. اظهرت المترابكات النانويه فعالية عالية في تثبيط نمو الخلايا لسرطان الرئة مقارنة بالخلائط المحضرة.

\*Email: [maha.aw.y@ihcoedu.uobaghdad.edu.iq](mailto:maha.aw.y@ihcoedu.uobaghdad.edu.iq)

## 1. Introduction

Cancer poses a significant global health challenge, as both incidence and mortality rates have risen in recent decades. Developing targeted and effective anticancer therapies remains an urgent priority. Conventional modalities like surgery, radiation therapy, immunotherapy and hormonal treatments are commonly employed. However, chemotherapy - the use of chemical agents to treat cancer - also plays a vital role, often in combination with other approaches. While chemotherapy can successfully kill cancer cells, systemic administration also affects healthy tissues, resulting in adverse side effects [1]. Seeking to improve chemotherapy outcomes, considerable research efforts have focused on engineered drug delivery systems capable of selectively transporting anticancer agents to tumor sites. This strategy aims to enhance therapeutic efficacy while reducing off-target impacts, addressing a critical unmet need given the growing cancer burden worldwide. One of the major challenges limiting chemotherapy effectiveness is the development of drug resistance in cancer cells. As a potential strategy to overcome resistance, researchers have increasingly investigated co-delivery systems that can concurrently administer two or more anti-cancer agents [2]. Polymer-nanocomposite materials have emerged as promising nanocarriers for biomedical applications such as drug delivery due to their tunable properties. Nanocomposites, synthesized by incorporating nanoscale fillers into polymer matrices, exhibit enhanced and customizable features compared to constituent polymers alone. Their applicability spans nanomedicine, tissue engineering and antimicrobial technologies among others. As drug delivery vehicles, polymer nanocomposites show potential for cancer treatment owing to capabilities such as controlled multi-drug release and targeted accumulation at tumor sites [3]. Leveraging nanotechnology, optimized co-delivery platforms may help address the pressing issue of resistance and improve chemotherapy outcomes against difficult-to-treat cancers. Polyvinyl alcohol (PVA) is a polyhydroxy water-soluble polymer with a two-dimensional hydrogen-bonded network film structure. PVA is a polymer that is semi-crystalline and has both crystalline and amorphous phases [4]. PVA is an excellent hydrophilic polymer with exceptional physicochemical properties, nontoxicity, and biocompatibility [5]. polyoxometalates (POMs), macroanionic groups in which an oxygen bridge binds the metal ions in their highest oxidation states [6]. Because of their unique properties and reactivity, they have been investigated in a number of fields, that involve catalysis, material science, drug development, medicine, and biosensors [7]. POMs have attracted much attention in recent years in pharmaceutical research as possible therapeutic agents such as anti-cancer, antibacterial, and antiviral drugs. They seem to have a particularly good probability of being widely considered as therapies in the near future [8] because of their low-cost cost of production, easy synthesis, fast modification, and other important properties. Polyvinylpyrrolidone (PVP) in the pharmaceutical industry, is a potential candidate for drug delivery applications due to its non-toxic, bio-inert, and hydrophilic properties. Its ability to form complexes with a variety of smaller molecules makes it suitable for the improvement of the bioavailability and sustained release of drugs from drug conjugated polymeric matrices [9].

Nanotechnology holds immense promise for advancing materials science through precisely manipulating matter at the nanoscale level of 1-100 nm. At this dimension, materials exhibit unique properties divergent from their bulk forms due to quantum mechanical effects. Gold nanoparticles (AuNPs) in particular have widespread applicability across diverse fields such as biomedical research [10]. As AuNPs are biocompatible, non-toxic and can be readily synthesized, they represent one of the most commonly investigated types of metallic nanoparticles. Their tunable size- and shape-dependent optical features have enabled applications including drug/gene delivery, imaging, and photothermal cancer therapy.

Moreover, AuNP surfaces allow facile conjugation with targeting ligands, facilitating functionalization for specialized biomedical applications. Due to these advantageous traits, AuNPs offer an attractive nanotechnological platform for developing innovative diagnostic and therapeutic systems at the nanoscale. Gold nanoparticles have witnessed significant developments in their use in biological applications, either used alone or in conjunction with other types of nanoparticles for the delivery of drugs, photothermal therapy, or as diagnostic tools in a variety of medical applications [11]. Silver nanoparticles (AgNPs) are the most well-known and widely used nanoparticulate material and have different catalytic, electric, and antibacterial properties [12,13]. The addition of nanoparticles enhanced the mechanical, thermal, optical, and antibacterial properties of nanocomposites [14]. The aim of this study is to investigate the influence of the gold and silver nano particles on the anticancer activity of the prepared compounds.

## 2. Experimental

### 2.1 Preparation of the poly acetal

All the used synthetic compounds were purchased from CHEM-LAB, Fluka, HIMEDIA, Aldrich and CDH companies. To prepare poly acetal, poly vinyl alcohol (PVA) (1g) was dissolved in 25 mL of di methyl sulfoxide (DMSO) and stirred for 30 minutes at room temperature. Para nitro benzaldehyde (1g) was dissolved in 20 mL of ethanol with 3 drops of concentrated  $H_2SO_4$  and stirred for 30 minutes at  $50\text{ }^\circ\text{C}$  temperature. The mixture of para nitro benzaldehyde and polyvinyl alcohol was heated for 9 hours with reflux at a temperature of  $50\text{ }^\circ\text{C}$  with stirring. A few drops of (1N) NaOH solution were added to the produced mixture to adjust the pH level to 7. The product was filtered after cooling, and it was then dried for 24 hours at  $50\text{ }^\circ\text{C}$  in an oven [15]. The synthesis of polyacetal (PA) is shown in Figure 1.

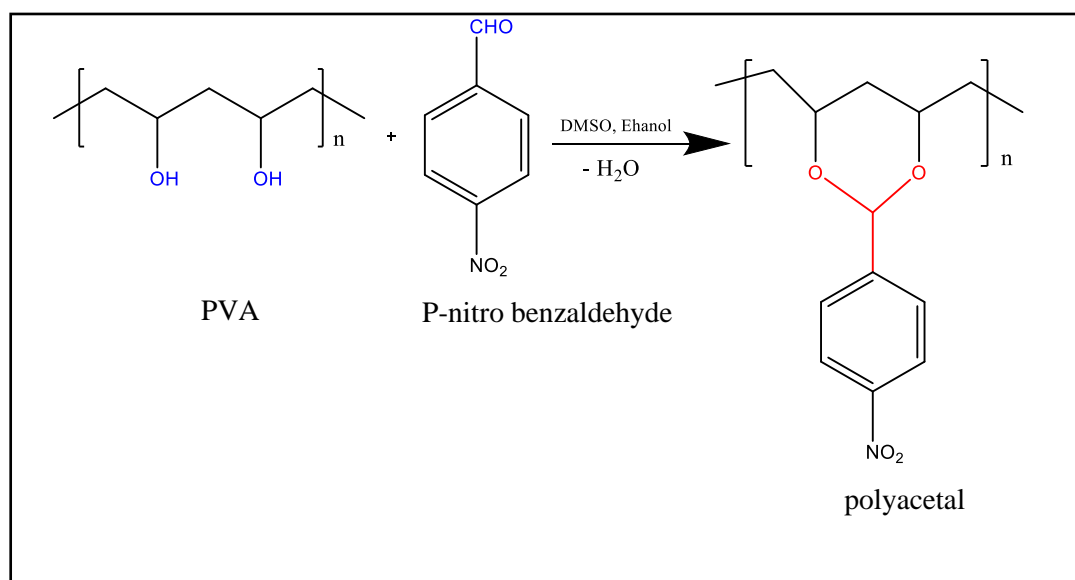


**Figure 1:** The preparation steps of poly cyclic acetal

### 2.2 Polymer blend preparation

The solution casting method in which the polymers were dissolved and mixed then the solvent was removed by drying to create a solid layer, was used to prepare polymer blends by dissolving the polyacetal and the PVP then mix them together as follows: 1 g of poly acetal was dissolved in 100 ml of DMSO with stirring at  $50\text{ }^\circ\text{C}$ , 5 g of PVP was dissolved in 100 ml of water to prepare a 5 wt% solution of the polymer and 15 and 10 ml of PA and 5 and 10 ml of PVP polymer were mixed to produce a homogenous solution for 30 minutes. The mixed

solution was poured into petri dishes and dried for 24 hours at 50 °C in the oven. Different ratios were mixed to prepare PA/PVP polymer blends [16].

### 2.3 Biosynthesis of gold and silver Nanoparticles

An onion peel crude extract was prepared as follows: 10 g of onion peel powder was mixed with 100 mL of deionized water. The mixture was heated to 50°C for 2 hours to facilitate extraction of active compounds from the powder. The heated solution was then filtered to remove insoluble material. The filtrate was dried in an oven at 50°C to obtain a powdered crude extract. For synthesis of gold nanoparticles using the extract, 0.01 g of the dried crude extract powder was dissolved in 100 mL of deionized water to make a 100-ppm onion peel extract solution. This extract solution served as both the reducing and stabilizing agent in the synthesis. The extract is known to contain polyphenolic compounds that can induce the reduction of gold ions to form gold nanoparticles when added to a chloroauric acid solution, as well as cap proteins and sugars that stabilize the formed nanoparticles [17].

For the preparation of  $\text{HAuCl}_4 \cdot 3\text{H}_2\text{O}$ ,  $\text{AgNO}_3$  Solutions, stock solutions were made by the following procedure: (1 g) of gold chloride trihydrate ( $\text{HAuCl}_4 \cdot 3\text{H}_2\text{O}$ ) was dissolved in 100 mL of deionized water. Then, 2 mL of the stock solution was taken and completed to 100 mL to prepare (100 ppm). By mixing (0.016g) of  $\text{AgNO}_3$  with (100 ppm) of deionized water in 100 mL,  $\text{AgNO}_3$  was prepared [18]. After 10 mL of gold chloride solution, 3 mL of aqueous onion peel extract, and silver nitrate were mixed, and the solution was then stirred for 10 minutes at 25 °C [18]. The color of the gold changed from yellow to purple, while the color of the silver changed from colorless to brown which confirm the formation of AuNPs and AgNPs. A centrifuge (10000 ppm) was used to separate the nanoparticles then the precipitate was taken and diluted with deionized water [18].

### 2.4 Preparation of Gold and Silver Nanocomposites

The nanocomposite film was synthesized as follows: 15 mL of poly acetal was combined with 5 mL of polyvinylpyrrolidone (PVP) in a container. Separately, gold nanoparticles (AuNPs) and silver nanoparticles (AgNPs) were prepared to a concentration of 100 ppm by reducing their respective salts. Then, 20 mL each of the AuNP and AgNP solutions were added to the poly acetal/PVP mixture. The combined components were stirred for two hours to ensure homogenization. Subsequently, the fully blended mixture was poured into petri dishes and allowed to dry at 50°C for 24 hours to form films [18].

### 2.5 Anticancer Activity

#### 2.5.1 Cell Cultures

The A1549 lung cancer cells were maintained in RPMI-1640 cell culture medium supplemented with 10% fetal bovine serum, 100 units/mL penicillin, and 100 µg/mL streptomycin to support cell growth. The cells were passaged using trypsin-EDTA, reseeded at 80% confluence, and grown at 37 °C twice weekly [19,20].

#### 2.5.2 Cytotoxicity Assays

The cytotoxic effects of polymer blends and nanocomposites were evaluated using 96-well plates and the MTT test [21,22]. In each well, 104 cells from each of the cell lines were planted. Cells were treated with nanocomposites in a range of concentrations after 24 hours or after the formation of a confluent monolayer. Cell viability was assessed 48 hours after the treatment by removing the medium, adding 28 L of an MTT solution containing 2 mg/mL, and incubating the cells for 2.5 h at 37 °C. Following removal of the MTT solution, the residual purple formazan crystals in each well were dissolved by adding 130 µL of dimethyl

sulfoxide (DMSO). The plates were then incubated for 15 minutes at 37°C with shaking to ensure full solubilization of the formazan crystals. The absorbance of each well was subsequently measured at 492 nm using a microplate spectrophotometer. The percentage of cytotoxicity, or the extent of inhibition of cell growth, was then calculated using the following formula that has been reported previously [24,25]:

$$\% \text{ Cytotoxicity} = (1 - \text{Absorbance of treated cells} / \text{Absorbance of untreated cells}) \times 100$$

Where the absorbance values correlate to the number of viable cells, with lower absorbance in treated wells indicating higher cytotoxicity from test materials. This quantitative assay thus allowed assessment of potential anti-proliferative effects of the synthesized nanomaterials. The inhibition rate was calculated using the equation  $(A-B/A \times 100)$ , where A represents the optical density of the control and B represents optical density of the samples [26]. The cells were poured into 24-well micro-titration plates at a density of  $1 \times 10^5$  cells mL<sup>-1</sup> and incubated for 24 h at 37 °C to assess the morphology of the cells under an inverted microscope. Later cells were treated with polymer blends and nanocomposites for 24 hours. The plates were then coated with crystal violet dye and they were then incubated at 37 °C for 10-15 min [24]. It required several mild washes with tap water to thoroughly remove the colour off the spot. A digital camera attached to the microscope was used to take pictures while the cells were being evaluated under an inverted microscope at a 100x magnification [27,28,29].

### 2.5.3 Statistical analysis

An unpaired t-test was utilized to statistically analyze the collected data in GraphPad Prism 6. The average and standard deviation of three measurements were used to present the results.

## 3. Results and Discussion

### 3.1 Scanning Electron Microscopy (SEM)

SEM microscopy was used to characterize the morphology and dimensions of the synthesized compounds, based on a prior reported method [30]. Figure 2 shows the SEM images of the polyacetal, PA/PVP blend, AuNPs, AgNPs, and Au,Ag nanocomposites. Figures 2A and 2B specifically depict the surface morphology of the AuNPs and AgNPs, respectively. Analysis of the SEM images revealed that the AgNPs exhibited an average diameter of 29.45 nm with a spherical shape, while the AuNPs had an average diameter of 41.61 nm and also appeared spherical in morphology.

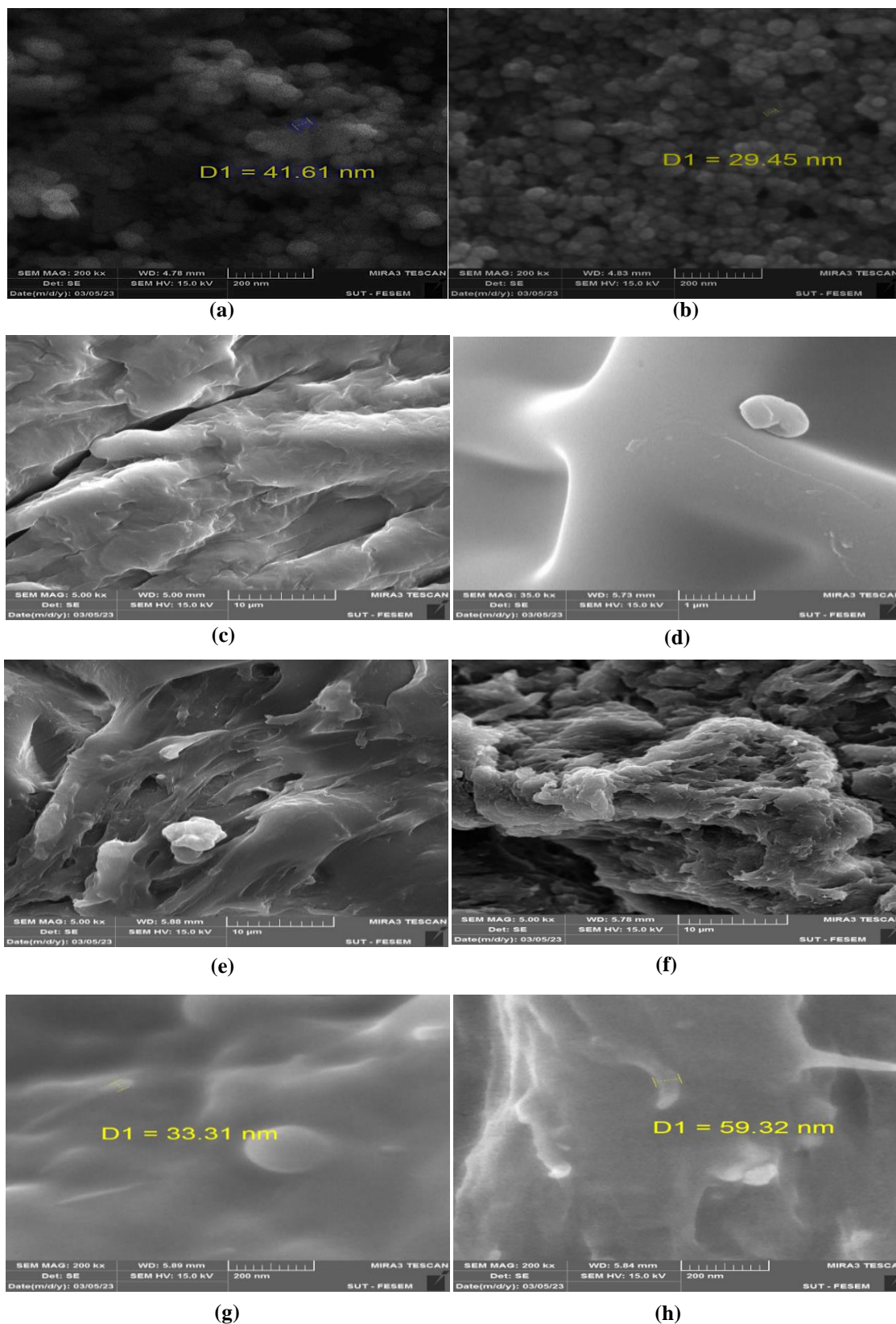


**Figure 2:** Scanning Electron Microscopy of (a- AuNPs) and (b- AgNPs) (c- polyacetal), (d- PVP), (e- polymer blend 1), (f- polymer blend 2), (g - Nanocomposite (PA/ PVP -AuNPs), (h- (PA/ PVP-AgNPs)

### 3.2 Analysis of X-ray diffraction (XRD)

AgNPs and AuNPs were evaluated for their crystallinity using X-ray diffraction (XRD) analysis. Figure 3a and b display the XRD results of the AuNPs and AgNPs that were prepared. The gold nanoparticles AuNPs exhibited peaks at  $38^\circ$ ,  $44^\circ$ , and  $49^\circ$  that matched Bragg's planes (111), (200), and (220), respectively, demonstrated that the AuNPs had a face-centered cubic structure. In accordance with (JCPDS 04-0784), AgNPs likewise showed a 2theta degree ranging from 10 to 80 [31]. According to (JCPDS 04-0783), the peak for AgNPs produced at 2theta values  $38^\circ$ ,  $49^\circ$ , and  $69^\circ$  corresponds to Bragg's reflection (200), (200), and (220), respectively [32].

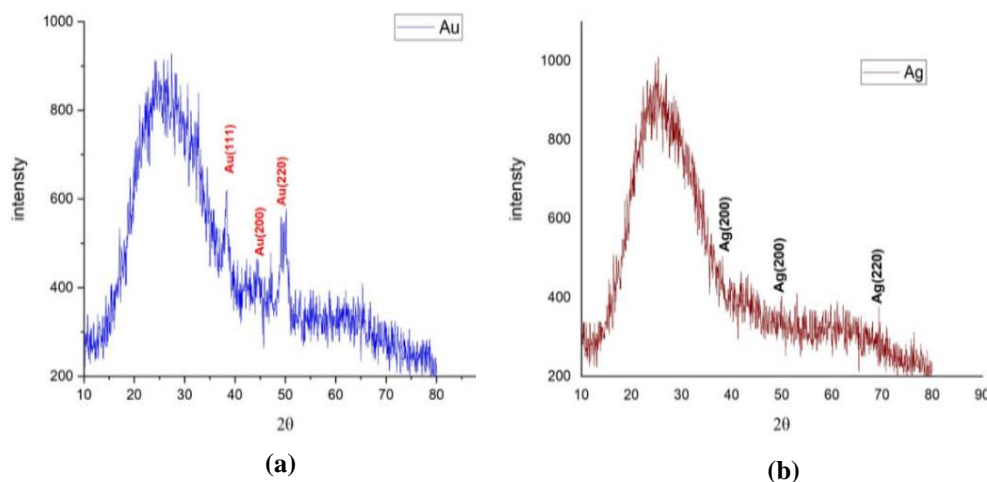
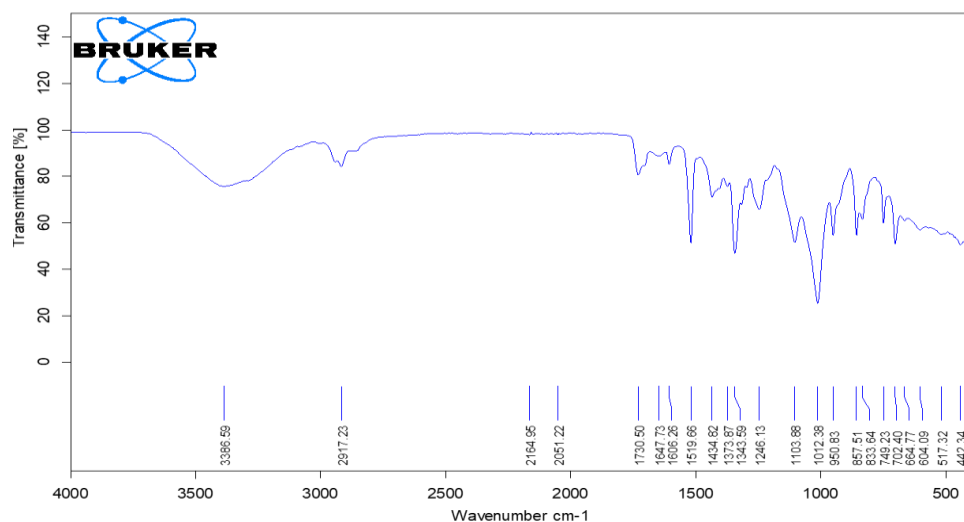


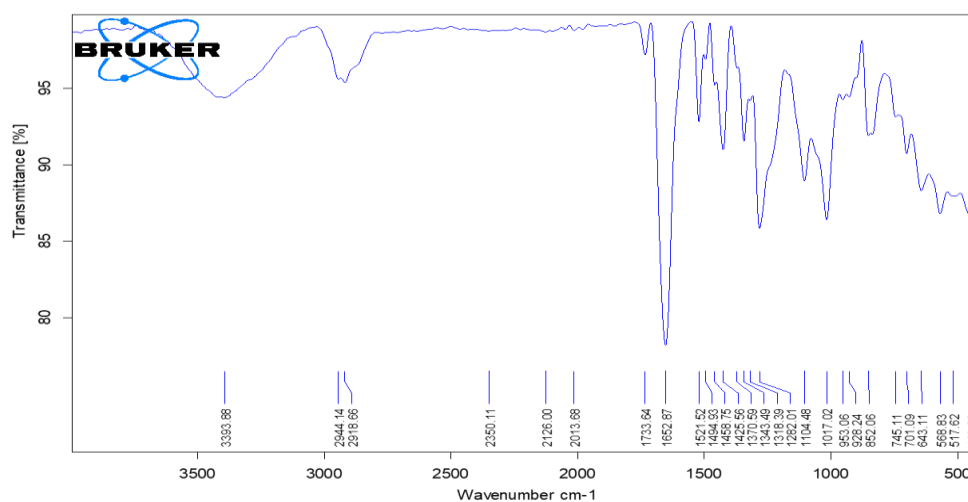
**Figure 3:** The (A-AuNPs) and (B-AgNPs) XRD patterns.

### 3.3 Characterization of Polyacetal, PVP, Polymer blend FT-IR Analysis

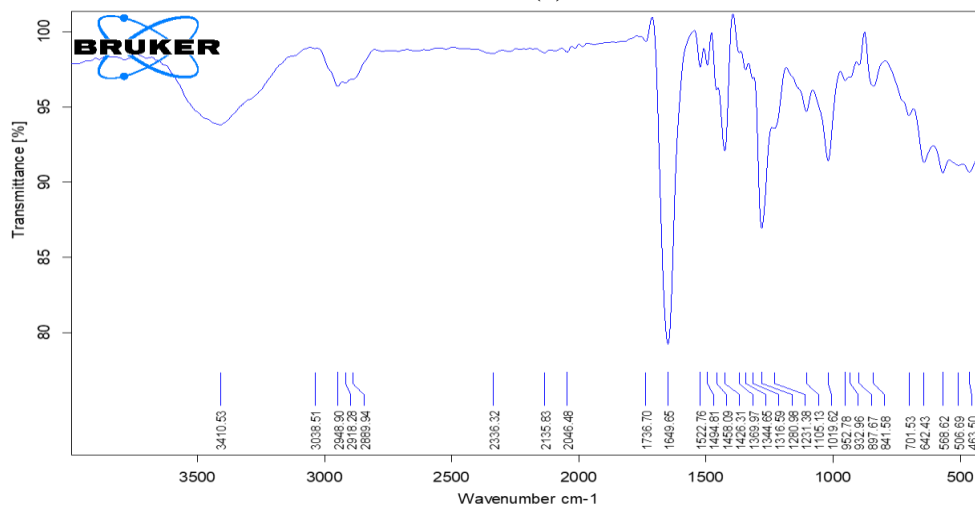
Figure 4A shows the polyacetal FT-IR spectrum, which is assigned as follows: The broad band is attributed to the vibrations of (OH stretching vibration) at  $3386\text{ cm}^{-1}$ , (C-H symmetric stretch) at  $2917\text{ cm}^{-1}$ , (C=C) at  $(1606, 1434)\text{ cm}^{-1}$ , (C=C), (C-O-C bending vibration), at  $1103\text{ cm}^{-1}$ , and (C-H are stretching vibration), at  $950\text{ cm}^{-1}$ . The PVP FTIR spectrum Figure 4B had a peak at  $3423\text{ cm}^{-1}$ , which indicates O-H stretching. Vibrational bands corresponding to C-H bending and  $\text{CH}_2$  wagging of the pyridine ring were observed at  $1425\text{ cm}^{-1}$  and  $1278\text{ cm}^{-1}$ , respectively. Peaks attributed to  $\text{CH}_2$  rocking and N-C=O bending were also identified at  $1016\text{ cm}^{-1}$  and  $567\text{ cm}^{-1}$ , respectively [33]. Figure 4C FTIR spectrum for the prepared polymer blend revealed a broad band at  $3393\text{ cm}^{-1}$ , which was attributed to the stretching vibration of PVP's hydroxyl group (OH). The existence of a hydroxyl group (OH) is demonstrated by the band at about  $1017\text{ cm}^{-1}$ . A pyridine ring (C=N)-related band appeared at  $1458\text{ cm}^{-1}$  [34].



(a)



(b)

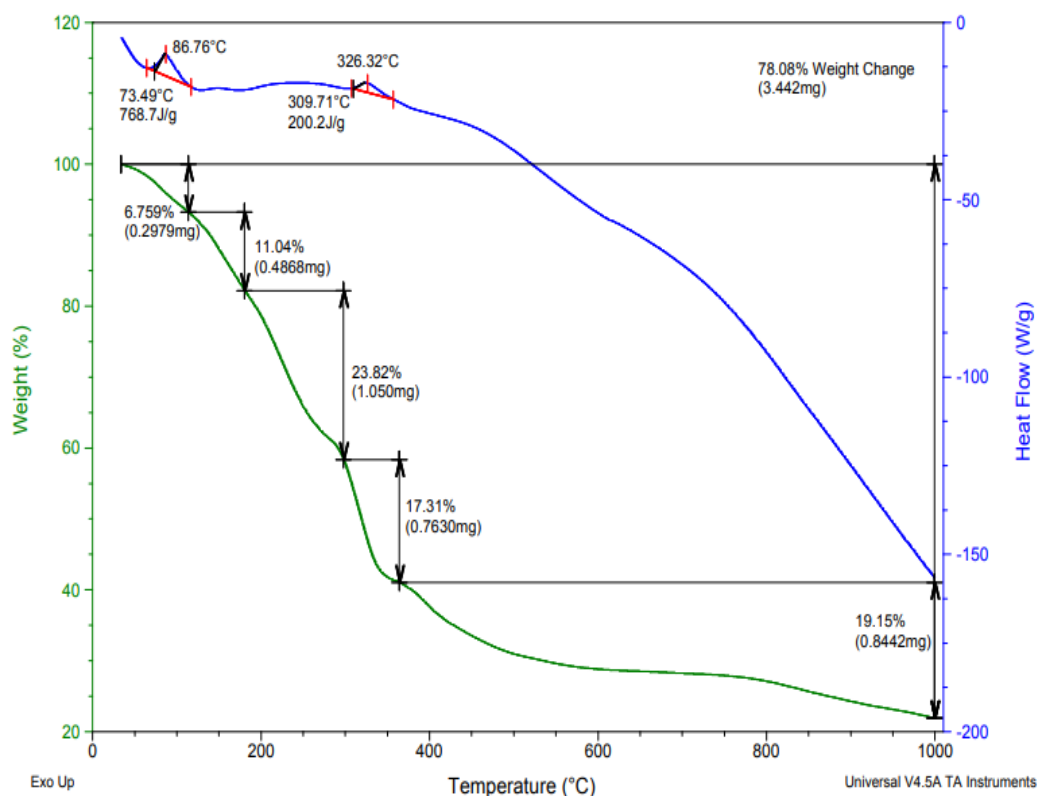


(c)

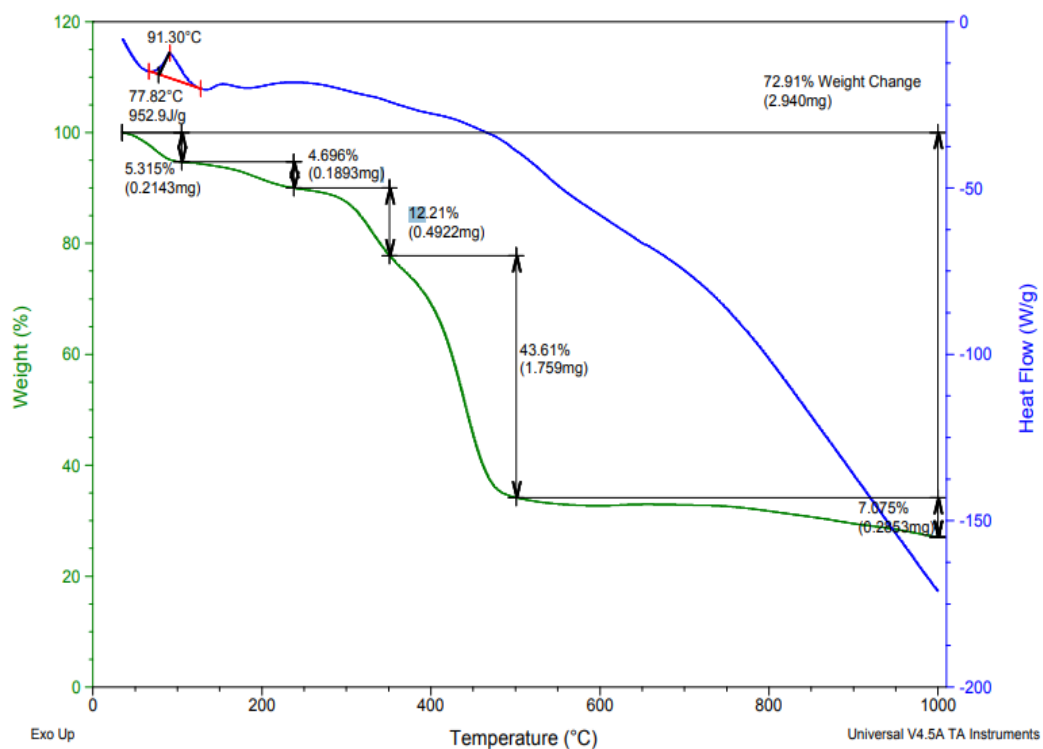
Figure 4: FTIR Spectrum(a-polyacetal), (b- PVP), (c- polymer blend)

### 3.4 Thermal Analysis (TGA, DSC)

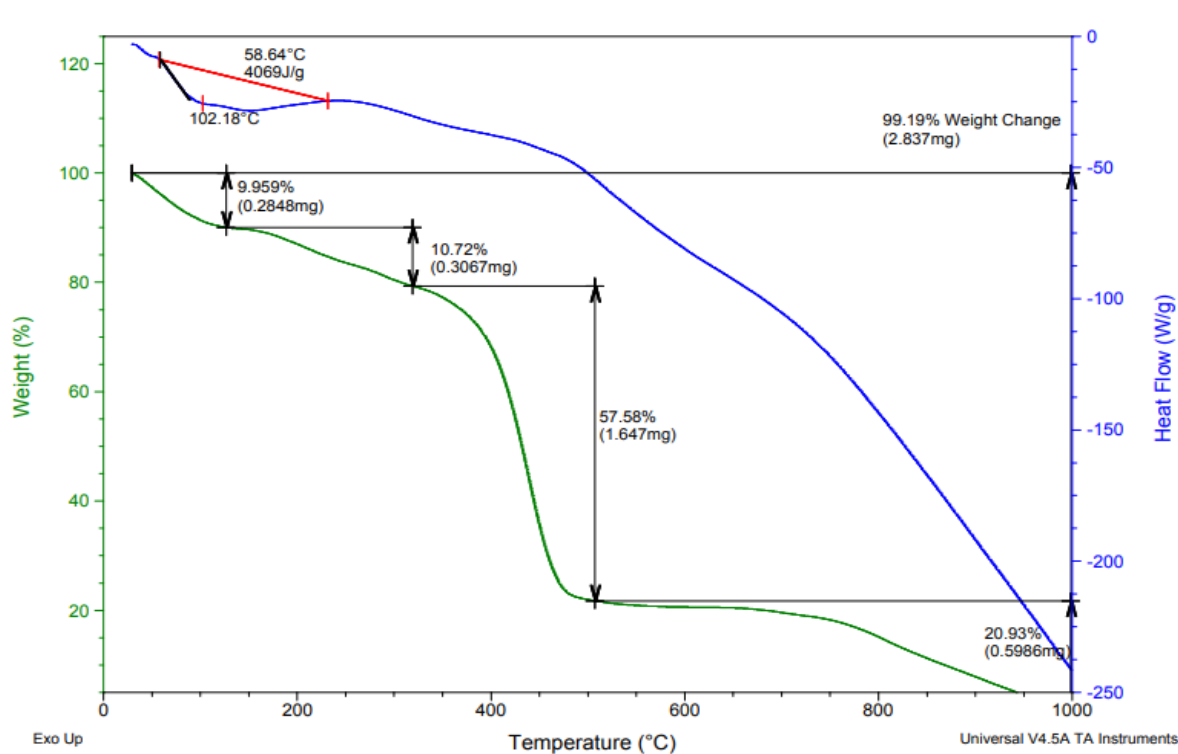
The thermogravimetric analysis and differential scanning calorimeter (TGA, DSC) has been used to analyze PVA, PVP, Polyacetal, PA/PVP polymer blend, and PA/PVP Au, Ag nanocomposites at temperatures ranging from 25°C to 1000°C at a constant rate of 10C°/ min. Figure 5a shows the polyacetal TGA curve. TG analysis revealed mass loss occurred in five stages as shown in Figure 5a. The initial stage from room temperature to 100°C resulted in a mass decrease of 6.759% corresponding to evaporation of volatile compounds in the sample. The second stage from 100-200°C showed an approximate mass loss of 11.04%. From 200-400°C (third stage), mass declined by around 23.82% associated with further decomposition. Between 400-500°C (fourth stage), a mass reduction of approximately 18.29% was attributable to decomposition of side groups. Finally, the fifth stage above 500°C exhibited roughly 19.15% mass loss linked to polymer chain degradation [35]. The accompanying DSC curve in Figure 5a identified the glass transition temperature (T<sub>g</sub>) of polyacetal as 86.76°C. A melting endothermic peak was also observable at 326.32°C, relating to the melting temperature (T<sub>m</sub>) of the polymer. These thermal analyses provided important physicochemical characterization of the synthesized nanocomposite [36]. The TGA curve of the PA/PVP polymer blend in Figure 5b showed five stages of mass loss, the first of which had a mass loss of (-5.315%). The second stage showed an approximate weight loss of (-4.696%), the third stage showed an approximate weight loss of (-12.21%), the fourth stage showed an approximate weight loss of (-43.61%), and the fifth stage showed an approximate weight loss of (-7.075%). The PA/PVP polymer blend's DSC curve in Figure 5b showed a T<sub>g</sub> of (91.30°C). The TGA curve for the PA/PVP-Au nanocomposite in Figure 5c showed four stages of mass loss, the first of which had a mass loss of (-9.959%). The second stage showed an estimated weight loss of (-10.72%), the third stage showed an approximate weight loss of (-57.58%), and the fourth stage showed an approximate weight loss of (-20.93%). The PA/PVP-Au nanocomposite's DSC curve in Figure 5c showed a T<sub>g</sub> of (102.18°C). The PA/PVP-Ag Nanocomposite Figure 5d TGA curve showed five phases of mass loss, the first of which had a mass loss of (-10.11%). TG analysis of the PA/PVP-Au nanocomposite revealed mass loss occurred in five stages, as shown in Figure 5b. The second stage from 100-200°C exhibited an average mass decrease of 7.847%. From 200-300°C (third stage), the average mass loss was approximately 15.60%. In the range of 300-500°C (fourth stage), an average mass reduction of about 38.50% took place. The final stage above 500°C showed an average mass decline of around 25.37%. For the PA/PVP-Ag nanocomposite (Figure 5d), the DSC curve identified the glass transition temperature (T<sub>g</sub>) as 104.95°C and melting temperature (T<sub>m</sub>) as 465.21°C. All thermal values were relatively higher compared to the individual components, demonstrating that polymer blending and metal nanoparticle coordination improved the thermal stability, likely through enhanced interactions imparting rigidity to the nanocomposites. These results indicate the successful fabrication of thermally stable nanocomposites for applications requiring resistance to elevated temperatures. It has also been noted that the blend film only exhibits one T<sub>g</sub> on its thermogram. This shows that the PA and PVP polymers are well blended together and that there are hydrogen bonding interactions between them in the blend. These results suggest that Nano-Au & Ag can enhance the thermal stability of nanocomposites at such a very low concentration, as illustrated in Figure 5.



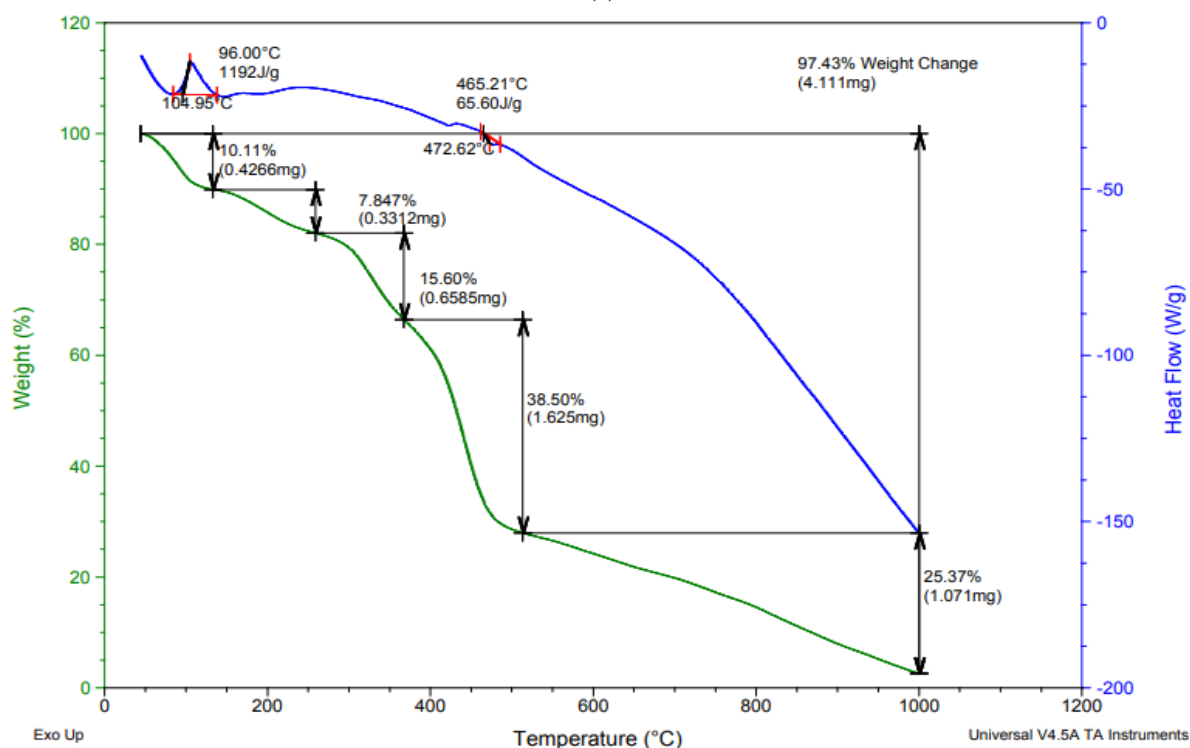
(a)



(b)



(c)

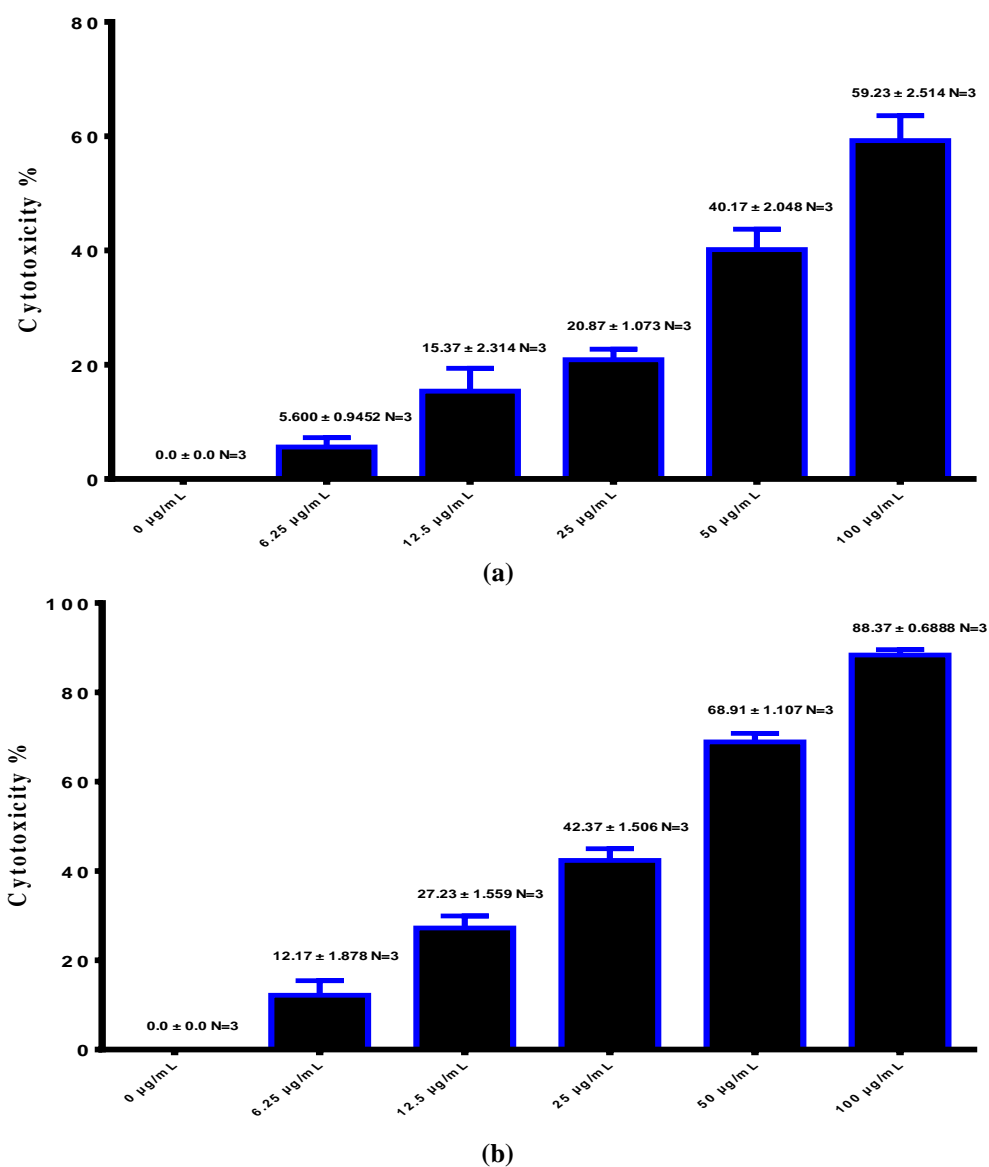


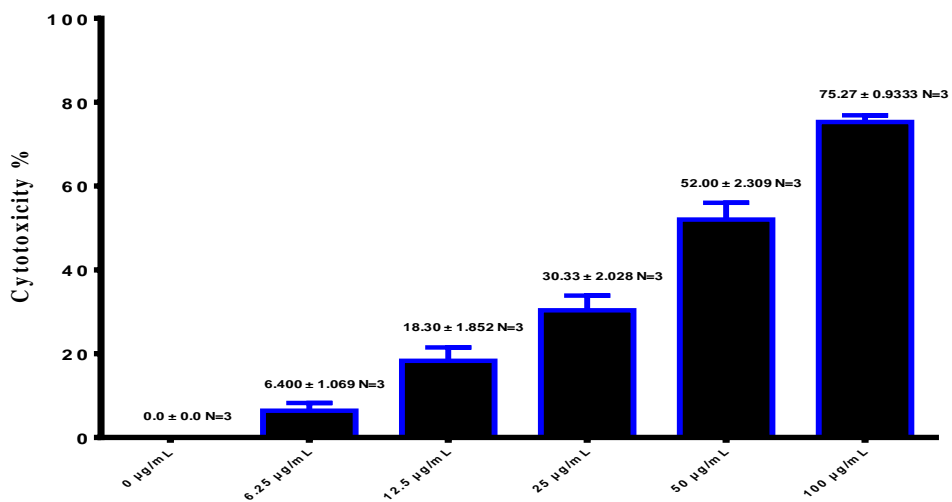
(d)

**Figure 5:** Thermal analysis (TGA, DSC) (a- Polyacetal), (b- Polymer blend), (c- Nanocomposite (PA / PVP -AuNPs)), (d- Nanocomposite (PA/ PVP -AgNPs)).

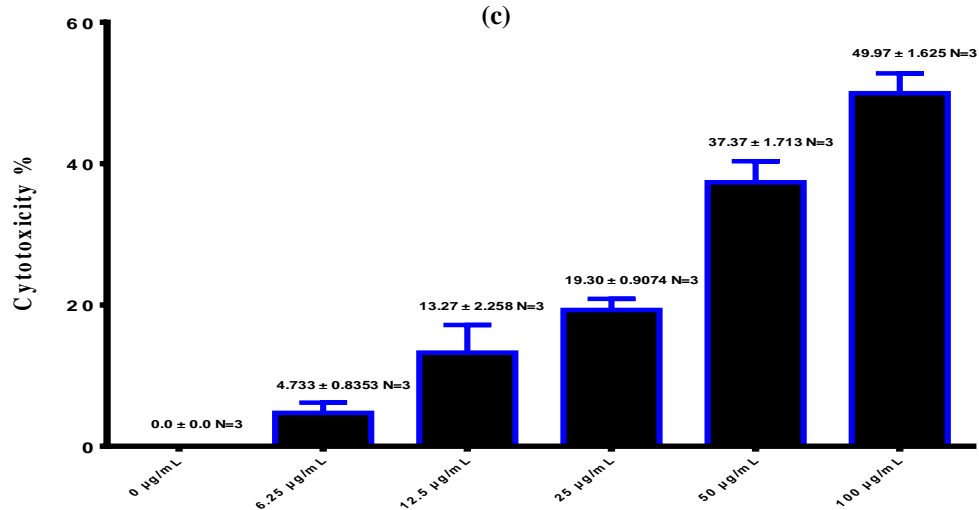
### 3.5 Anticancer cell line

Polymer blend, Nanocomposites' cytotoxic effect on cancer cells was investigated. To assess the blend's anticancer efficiency, nanocomposites were tested for their ability to inhibit the growth of the lung cancer cell line A1549. Figures 6, 7 & 8 from the results of this research demonstrate that blends of nanocomposites had a very significant cytotoxic effect against human cancer cell lines. The results demonstrate that blends and nanocomposites can inhibit cell line growth, and that this effect is concentration dependent. Through aggregation and trapping, the nanoparticles' NPs direct affect the tumor cells. The process further defined by the retention and penetration effect that irregular lymphatic flow and angiogenic vessels impose on cancerous cells. As a result, when compared to normal cells, these NPs accumulate more or more specifically inside cancerous cells. The results indicated that Nanocomposites have more inhibition effect than the polymer blend. Results indicated cytotoxic effect on A1549 cells, with  $IC_{50}$  values of 35.78 g/mL for (a), 20.62 g/mL for (b), and 25.92 g/ml for (c), and 38.05  $\mu$ g/mL for (d), and 22.09  $\mu$ g/mL for (e), and 28.43  $\mu$ g/mL for (f) [37]. As shown in Figure 6.

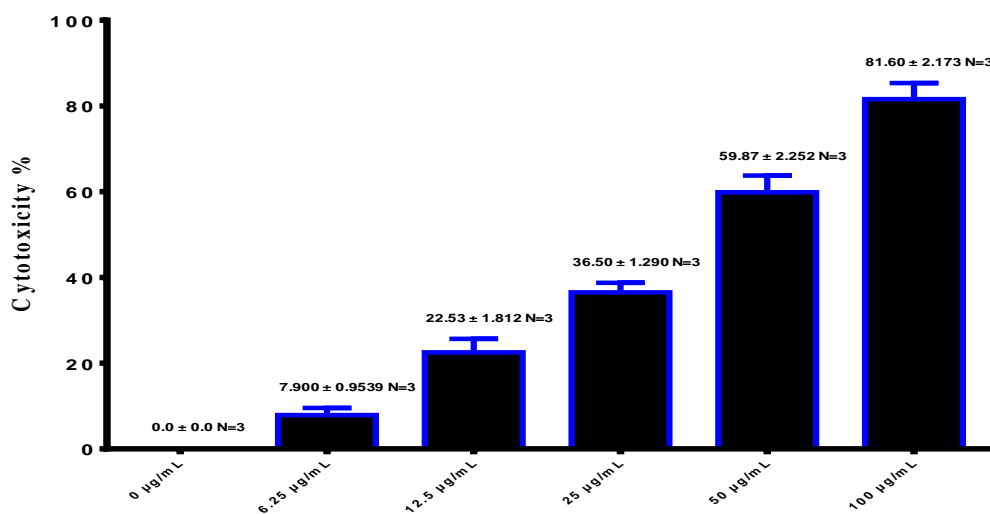




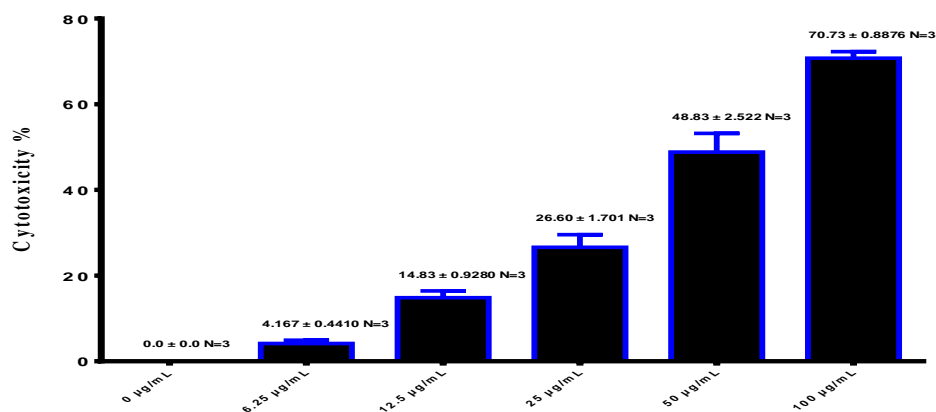
(c)



(d)



(e)



(f)

**Figure 6:** Effect of polymer blends and nanocomposite materials (gold, silver) on cells (a) Polymer blend1 A1549 cells. (b) Nanocomposite PA/ PVP -AuNPs A1549 undergo morphological alterations after being treated with Nanocomposite (Gold 100 ppm). (c) Nanocomposite (PA/ PVP -AgNPs) A1549, (d) Polymer blend2 A1549 cells. (e) Nanocomposite PA/ PVP -AuNPs A1549 undergo morphological alterations after being treated with Nanocomposite (Gold 100 ppm). (f) Nanocomposite (PA/ PVP -AgNPs) A1549 cells undergo morphological alterations after being treated with Nanocomposite (Silver 100 ppm) cells undergo morphological alterations after being treated with Nanocomposite (Silver 100 ppm).

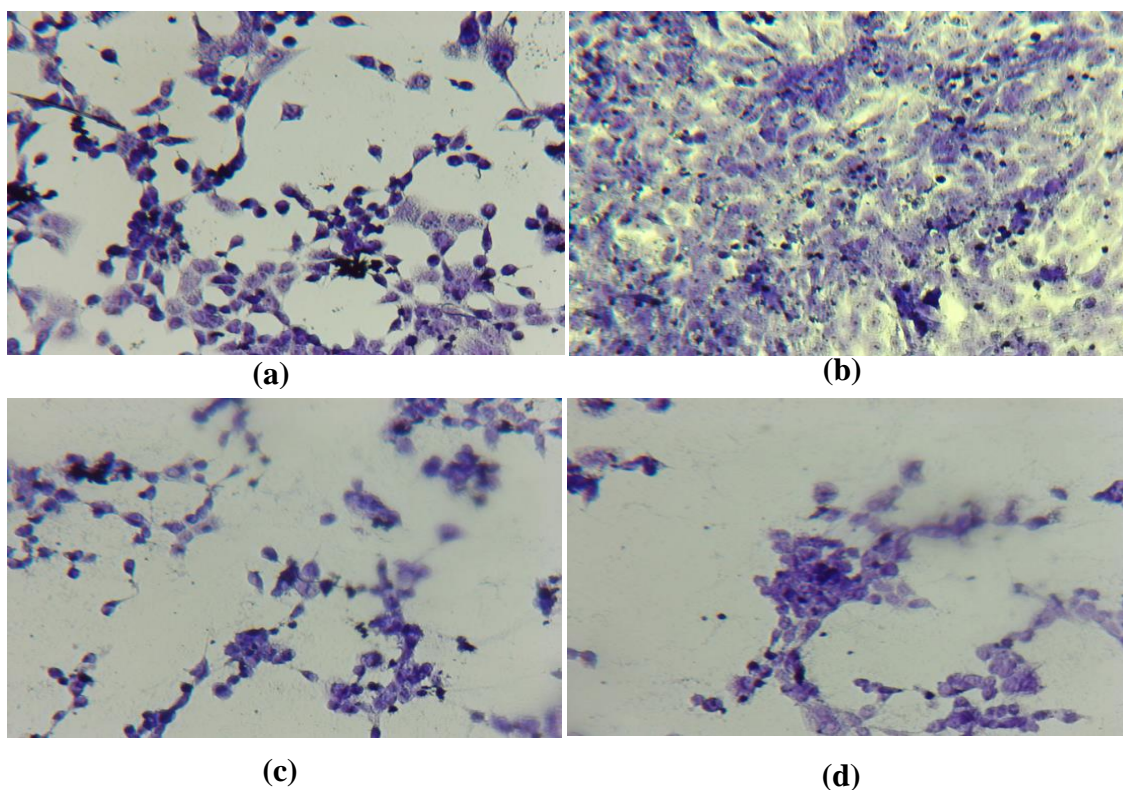


**Figure 7:** A1549 cell morphology after treatment with polymer blend 1 and its nanocomposites (a- Control) (b- Polymer blend1), (c- Nanocomposite PA/ PVP –AuNPs), (d- Nanocomposite PA/ PVP -AgNPs)

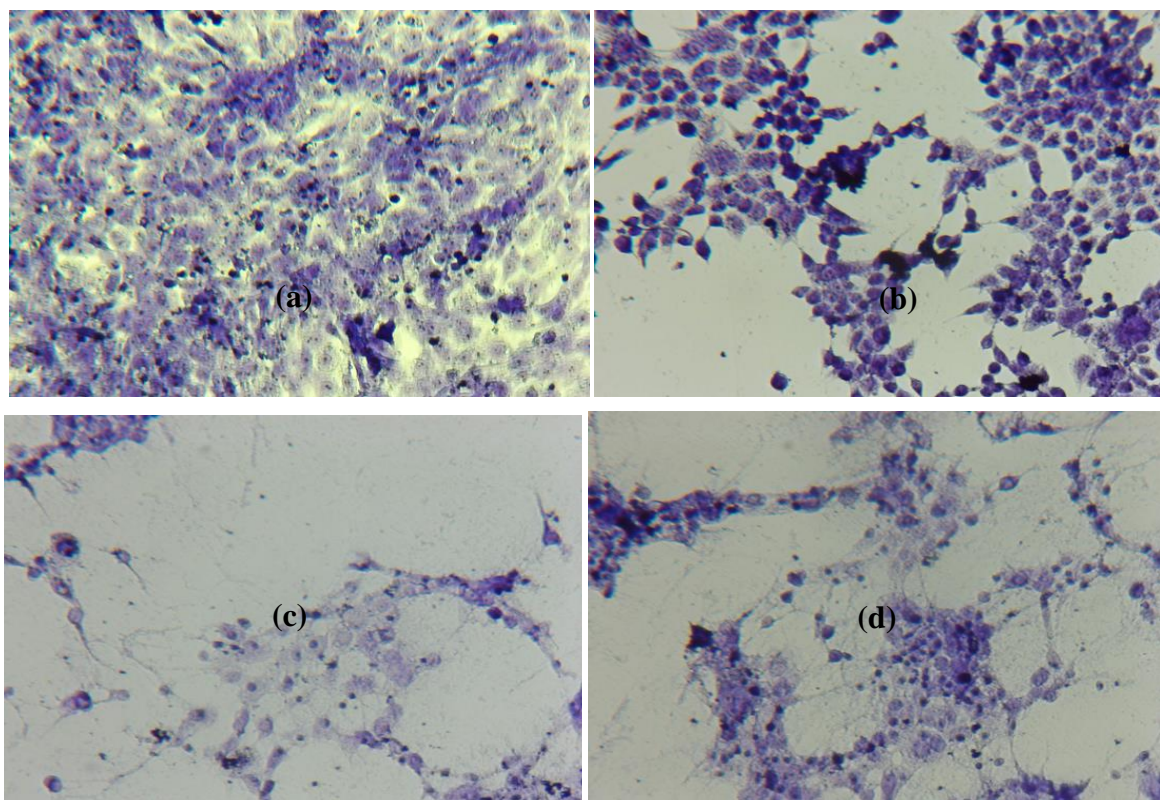


**Figure 8:** A1549 cell morphology after treatment with polymer blend 2 and its nanocomposites (a- Control) (b- Polymer blend2), (c- Nanocomposite PA/ PVP –AuNPs), (d- Nanocomposite PA/ PVP -AgNPs)

### Conclusion

In this work, the anticancer activities of the prepared polyacetal, PA/PVP polymer blend with different ratios, gold & silver nanocomposites were investigated. The obtained compounds were studied by FT-IR, SEM, DSC-TGA and XRD spectroscopy. The anticancer activity of the nanocomposites against the A1549 lung cancer cell line was evaluated. The results revealed that due to the presence of Au and Ag nanoparticles, the activity increased toward the A1549 lung cancer cell line, and that nanocomposites have demonstrated more anticancer activity than polymer blends.

### Acknowledgment

We extend our thanks to the Department of Chemistry, College of Education for pure science / Ibn Alhaitham, University of Baghdad, for their assistance in completing the research.

### References

- [1] Z. Chaudhary, N. Ahmed, A. ur. Rehman, and G. M. Khan, "Lipid polymer hybrid carrier systems for cancer targeting: A review", *International Journal of Polymeric Materials and Polymeric Biomaterials*, vol. 67, no. 2, pp. 86-100, 2018.
- [2] N. Li, L. Zhao, L. Qi, Z. Li, and Y. Luan, "Polymer assembly: Promising carriers as co-delivery systems for cancer therapy", *Progress in Polymer Science*, vol. 58, pp. 1-26, 2016.
- [3] S. Thakur, P. K. S. Malviya, "Utilization of Polymeric Nanoparticle in Cancer Treatment. A Review", *J. Pharm. Care Health Syst.*, vol.4, no. 2, pp.172, 2017.

- [4] A. H. Samir, R. S. Saeed, and F. S. Matty, "Synthesis and Study of Modified Polyvinyl Alcohol Containing Amino Acid Moieties as Anticancer Agent", *Oriental Journal of Chemistry*, vol. 34, no. 1, pp. 286, 2018.
- [5] E. N. Talib and M. A. Younus, "Preparation, Characterization and Antimicrobial activity of Chitosan Schiff base / Polyvinyl Alcohol Nanocomposite", *Journal of Global Pharma Technology*, vol. 11, no. 9, pp. 87-92, 2019.
- [6] H. K. Yang, Y.-X. Cheng, M.-M. Su, Y. Xiao, M.-B. Hu, W. Wang, et al., "Polyoxometalate–biomolecule conjugates: A new approach to create hybrid drugs for cancer therapeutics", *Bioorg. Med. Chem. Let.*, vol. 23, no. 5, pp. 1462-1466, 2013.
- [7] D. Karimian, B. Yadollahi, and V. Mirkhani, "Dual functional hybrid-polyoxometalate as a new approach for multidrug delivery", *Micropor. Mesopor. Mat.*, vol. 247, pp. 23-30, 2017.
- [8] A. Bijelic, M. Aureliano, and A. Rompel, "Polyoxometalates as potential next-generation metallodrugs in the combat against cancer", *Ang. Chem. Int. Ed.*, vol. 58, no. 10, pp. 2980-2999, 2019.
- [9] A. Hasan, G. Waibhaw, S. Tiwari, K. Dharmalingam, I. Shukla, and L. M. Pandey, "Fabrication and characterization of chitosan, polyvinylpyrrolidone, and cellulose nanowhiskers nanocomposite films for wound healing drug delivery application", *Journal of Biomedical Materials Research Part A*, vol. 105, no. 9, pp. 2391-2404, 2017.
- [10] M. C. Roco, C. A. Mirkin, and M. C. Hersam, "Nanotechnology research directions for societal needs in 2020: summary of international study", *Journal of Nanoparticle Research*, vol. 13, no. 3, pp. 897-919, 2011.
- [11] Y. Mikami, A. Dhakshinamoorthy, M. Alvaro, and H. Garcia, "Catalytic activity of unsupported gold nanoparticles", *Catalysis Science & Technology*, vol. 3, no. 1, pp. 58-69, 2013.
- [12] S. B. Yaqoob, R. Adnan, R. M. R. Khan, and M. Rashid, "Gold, silver, and palladium nanoparticles: a chemical tool for biomedical applications", *Frontiers in Chemistry*, vol. 8, pp. 376, 2020.
- [13] X. F. Zhang, Z. G. Liu, W. Shen, and S. Gurunathan, "Silver nanoparticles: synthesis, characterization, properties, applications, and therapeutic approaches", *International Journal of Molecular Sciences*, vol. 17, no. 9, pp. 1534, 2016.
- [14] B. M. Al-dabbag and H. J. Kadhim, "Nano composites of PAM Reinforced with Al<sub>2</sub>O<sub>3</sub>", *Baghdad Science Journal*, 2023.
- [15] E. Delattre, G. Lemiere, J. R. Desmurs, B. Boulay, and E. Duñach, "Poly (vinyl alcohol) functionalization with aldehydes in organic solvents: Shining properties of poly (vinyl acetals)", *Journal of Applied Polymer Science*, vol. 131, no. 17, 2022.
- [16] M. A. Younus, "Synthesis and Antibacterial Activity of PEG Polycyclic Acetal Metal Complex/PVA Polymer Blend Film", *Ibn AL-Haitham Journal For Pure and Applied Sciences*, vol. 33, no. 3, pp. 44-54, 2020.
- [17] M. A. Younus and B. F. Abdallaha, "Synthesis, Characterization and Anticancer Activity of Chitosan Schiff Base/PVP Gold Nano Composite in Treating Esophageal Cancer Cell Line", *Baghdad Science Journal*, 2023.
- [18] B. F. Abdallaha, M. A. Younus, and I. J. Ibraheem, "Preparation, Characterization, Antimicrobial and Antitumor Activity of Chitosan Schiff base/PVA/PVP Au, Ag Nanocomposite in Treatment of Breast Cancer Cell Line", *Nanomed Res J*, vol.6, no.4, pp. 369-384, Autumn 2021.
- [19] A. G. Al-Ziaydi, A. M. Al-Shammari, M. I. Hamzah, and M. S. Jabir, "Hexokinase inhibition using D-Mannoheptulose enhances oncolytic newcastle disease virus-mediated killing of breast cancer cells", *Cancer Cell International*, vol. 20, no. 1, pp. 1-10, 2020.

- [20] A. G. Al-Ziaydi, M. I. Hamzah, A. M. Al-Shammari, H. S. Kadhim, and M. S. Jabir, "The anti-proliferative activity of D-mannoheptulose against breast cancer cell line through glycolysis inhibition", *AIP Conference Proceedings*, vol. 2307, no. 1, pp. 020023, 2020.
- [21] R. I. Mahmood, A. A. Kadhim, S. Ibraheem, S. Albukhaty, H. S. Mohammed-Salih, R. H. Abbas, et al., "Biosynthesis of copper oxide nanoparticles mediated *Annona muricata* as cytotoxic and apoptosis inducer factor in breast cancer cell lines", *Scientific Reports*, vol. 12, no. 1, pp. 1-10, 2022.
- [22] A. G. Al-Ziaydi, M. I. Hamzah, A. M. Al-Shammari, H. S. Kadhim, and M. S. Jabir, "Newcastle disease virus suppress glycolysis pathway and induce breast cancer cells death", *VirusDisease*, 2020.
- [23] A. J. Jasim, G. M. Sulaiman, H. Ay, S. A. Mohammed, H. A. Mohammed, M. S. Jabir, and R. A. Khan, "Preliminary trials of the gold nanoparticles conjugated chrysin: An assessment of anti-oxidant, anti-microbial, and in vitro cytotoxic activities of a nanoformulated flavonoid", *Nanotechnology Reviews*, vol. 11, no. 1, pp. 2726-2741, 2022.
- [24] S. Al-Musawi, S. Albukhaty, H. Al-Karagoly, G. M. Sulaiman, M. S. Jabir, H. Naderi-Manesh, "Dextran-coated superparamagnetic nanoparticles modified with folate for targeted drug delivery of camptothecin", *Advances in Natural Sciences: Nanoscience and Nanotechnology*, vol. 11, no. 4, pp. 045009, 2020.
- [25] A. M. Al-Shammari, A. A. Al-Saadi, S. M. Al-Shammari, and M. S. Jabir, "Galangin enhances gold nanoparticles as anti-tumor agents against ovarian cancer cells", *AIP Conference Proceedings*, vol. 2213, no. 1, pp. 020206, 2020.
- [26] M. Jawad, K. Öztürk, and M. S. Jabir, "TNF- $\alpha$  loaded on gold nanoparticles as promising drug delivery system against proliferation of breast cancer cells", *Materials Today: Proceedings*, vol. 42, pp. 3057-3061, 2021.
- [27] Z. S. Abbas, G. M. Sulaiman, M. S. Jabir, S. A. Mohammed, R. A. Khan, H. A. Mohammed, and A. Al-Subaiyel, "Galangin/ $\beta$ -Cyclodextrin Inclusion Complex as a Drug-Delivery System for Improved Solubility and Biocompatibility in Breast Cancer Treatment", *Molecules*, vol. 27, no. 14, pp. 4521, 2022.
- [28] A. A. Ibrahim, M. M. Kareem, T. H. Al-Noor, T. Al-Muhimeed, A. A. AlObaid, S. Albukhaty, and U. I. Sahib, "Pt (II)-Thiocarbohydrazone complex as cytotoxic agent and apoptosis inducer in Caov-3 and HT-29 cells through the P53 and Caspase-8 pathways", *Pharmaceuticals*, vol. 14, no. 6, pp. 509, 2021.
- [29] A. M. Sameen, M. S. Jabir, and M. Q. Al-Ani, "Therapeutic combination of gold nanoparticles and LPS as cytotoxic and apoptosis inducer in breast cancer cells", *AIP Conference Proceedings*, vol. 2213, no. 1, pp. 020215, 2020.
- [30] V. Soshnikova, Y. J. Kim, P. Singh, Y. Huo, J. Markus, S. Ahn, et al., "Cardamom fruits as a green resource for facile synthesis of gold and silver nanoparticles and their biological applications", *Artificial Cells, Nanomedicine, and Biotechnology*, vol. 46, no. 1, pp. 108-117, 2018.
- [31] S. Rajeshkumar, "Anticancer activity of eco-friendly gold nanoparticles against lung and liver cancer cells", *Journal of Genetic Engineering and Biotechnology*, vol. 14, no. 1, pp. 195-202, 2016.
- [32] R. Pokrowiecki, J. Wojnarowicz, T. Zareba, I. Koltsov, W. Lojkowski, S. Tyski, and P. Zawadzki, "Nanoparticles and human saliva: A step towards drug delivery systems for dental and craniofacial biomaterials", *International Journal of Nanomedicine*, vol. 14, pp. 9235, 2019.

- [33] S. M. Al-Majidi and M. G. Al-Khuzai, "Synthesis and Characterization of New Azo Compounds Linked to 1,8-Naphthalimide and Studying Their Ability as Acid-Base Indicators", *Iraqi Journal of Science*, pp. 2341-2352, 2019.
- [34] R. Pokrowiecki, J. Wojnarowicz, T. Zareba, I. Koltsov, W. Lojkowski, S. Tyski, and P. Zawadzki, "Nanoparticles and human saliva: a step towards drug delivery systems for dental and craniofacial biomaterials", *International Journal of Nanomedicine*, vol. 14, pp. 9235-9257, 2019.
- [35] S. M. Abass, M. A. Wahab, H. S. Mohammed, and A. A. Hashim, "Study of rheological and mechanical properties of bitumen blended with two alpha phases of polyamide", *AIP Conference Proceedings*, vol. 2372, no. 1, pp. 130006, 2021.
- [36] B. J. Ahmed, M. H. Saleem, and F. S. Matty, "Synthesis and Study of the Antimicrobial Activity of Modified Polyvinyl Alcohol Films Incorporated with Silver Nanoparticles", *Baghdad Science Journal*, 2023.
- [37] A. Shah, A. A. Ashames, M. A. Buabeid, and G. Murtaza, "Synthesis, in vitro characterization and antibacterial efficacy of moxifloxacin-loaded chitosan-pullulan-silver-nanocomposite films", *Journal of Drug Delivery Science and Technology*, vol. 55, p. 101366, 2020.